

Cell Reports, Volume 40

Supplemental information

**Sensory neurons display cell-type-specific
vulnerability to loss of neuron-glia interactions**

Benayahu Elbaz, Lite Yang, Maia Vardy, Sara Isaac, Braesen L. Rader, Riki Kawaguchi, Maria Traka, Clifford J. Woolf, William Renthal, and Brian Popko

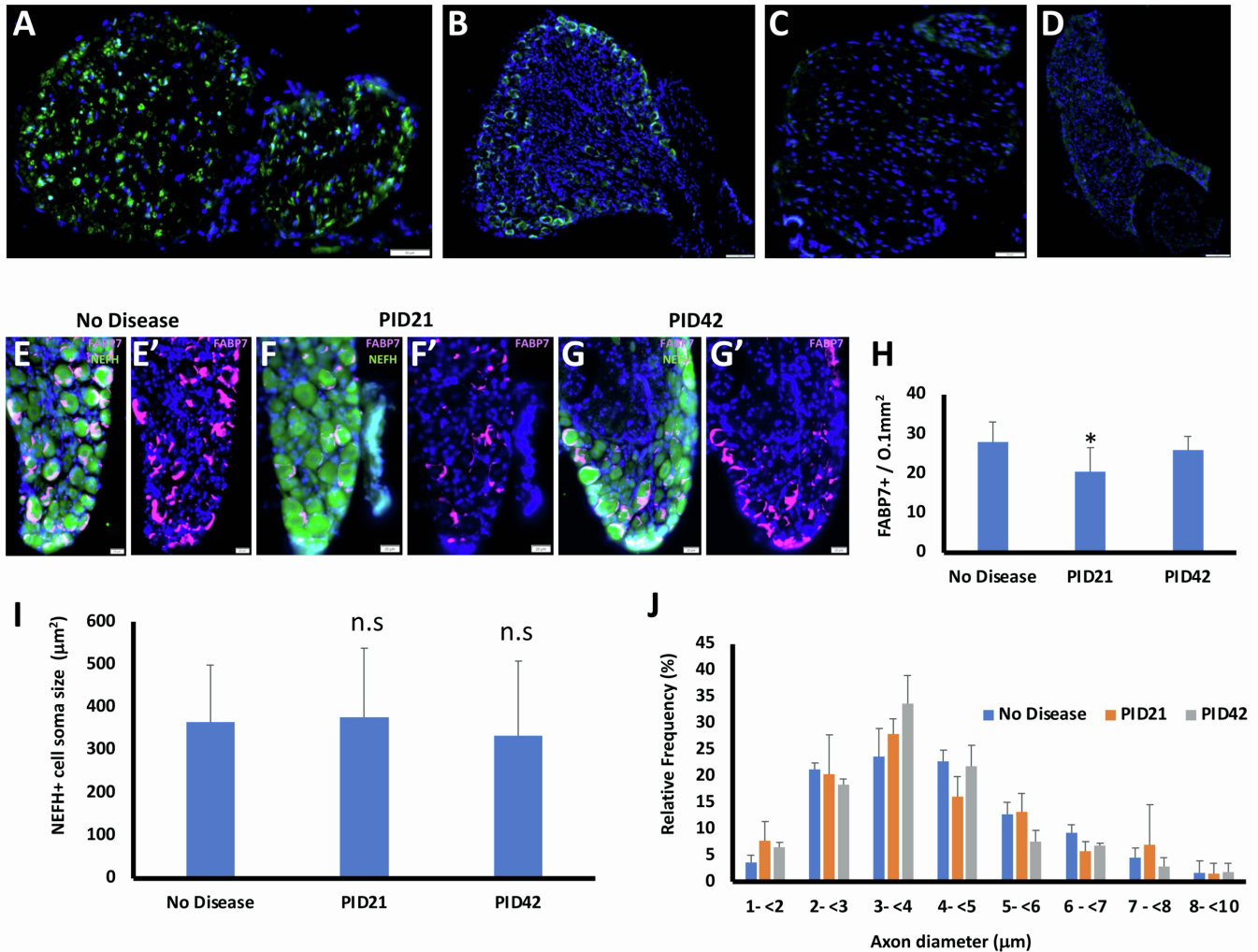


Figure. S1, related to figure 1: Ablation of satellite glial cells. (A-D) Eight-week-old Plp-CreERT;ROSA26-EYFP mice and Cre negative ROSA26-EYFP mice (used as control) were injected with tamoxifen, and the sciatic nerve and the L3-L5 DRGs were dissected. (A) In the sciatic nerve of the Plp-CreERT;ROSA26-EYFP mice, the expression of EYFP was detected by anti GFP antibody. (B) The expression of EYFP in the DRG of the Plp-CreERT;ROSA26-EYFP mice. (C) The expression of EYFP was not detected in the sciatic nerve of the ROSA26-EYFP mice. (D) The expression of EYFP was not detected in the DRG of the ROSA26-EYFP mice. n=3 for the Cre positive and the Cre negative mice. (E-G). Eight-week-old Plp-CreERT;ROSA26-eGFP-DTA mice and Cre negative ROSA26-eGFP-DTA mice (used as control) were injected with tamoxifen, and L3-L5 DRGs were dissected for IHC. The DRGs were labeled at No disease (E), at PID21 (F) and PID42 (G). (H) Statistically significant reduction in the density of FABP7 labelled cells at PID21. (I) No change in NEFH positive cell soma size. (J). No effect on axonal diameter

distribution in the sciatic nerve. For panels E-I n=3 for no disease, n=3 for PID21, and 3 for PID42.
For panel I, n=3 for no disease, n=4 for PID21, and 3 for PID42.

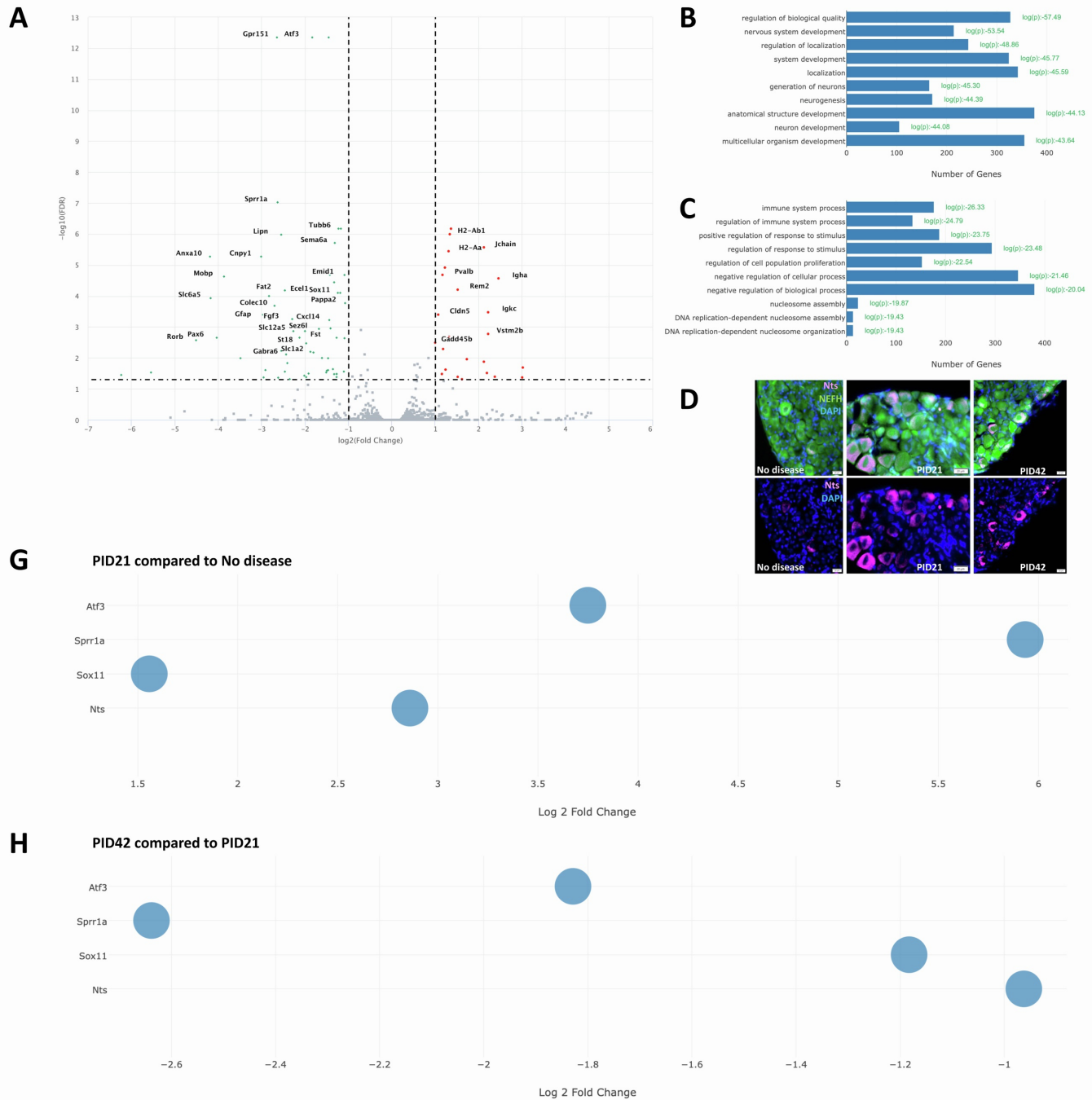


Figure. S2, related to figure 2: The expression of Regeneration Associated Genes in the DRG at PID42. Eight-week-old Plp-CreERT;ROSA26-eGFP-DTA mice and Cre negative ROSA26-eGFP-DTA mice (used as control) were injected with tamoxifen, and L3-L5 DRGs were dissected for bulk RNA-seq at PID21 and PID42. (A) Volcano plot of the Differentially Expressed Genes (DEG) in the DRG at PID42 compared to PID21. Green- downregulated genes, red-

upregulated genes. (B) Biological processes analysis of downregulated genes. (C) Biological processes analysis of upregulated genes. (D) Verification of NTS upregulation upon disease by IHC. (G) The expression of *Atf3*, *Sprr1a*, *Sox11* and *Nts* is upregulated at PID21 compared to no disease. (H) The expression of *Atf3*, *Sprr1a*, *Sox11* and *Nts* is downregulated at PID42 compared to PID21. n = 2 biologically independent experiments. (FDR \leq 0.05, fold-change \geq 2). For panel D, n=3 for no disease, n=3 for PID21, and 3 for PID42.

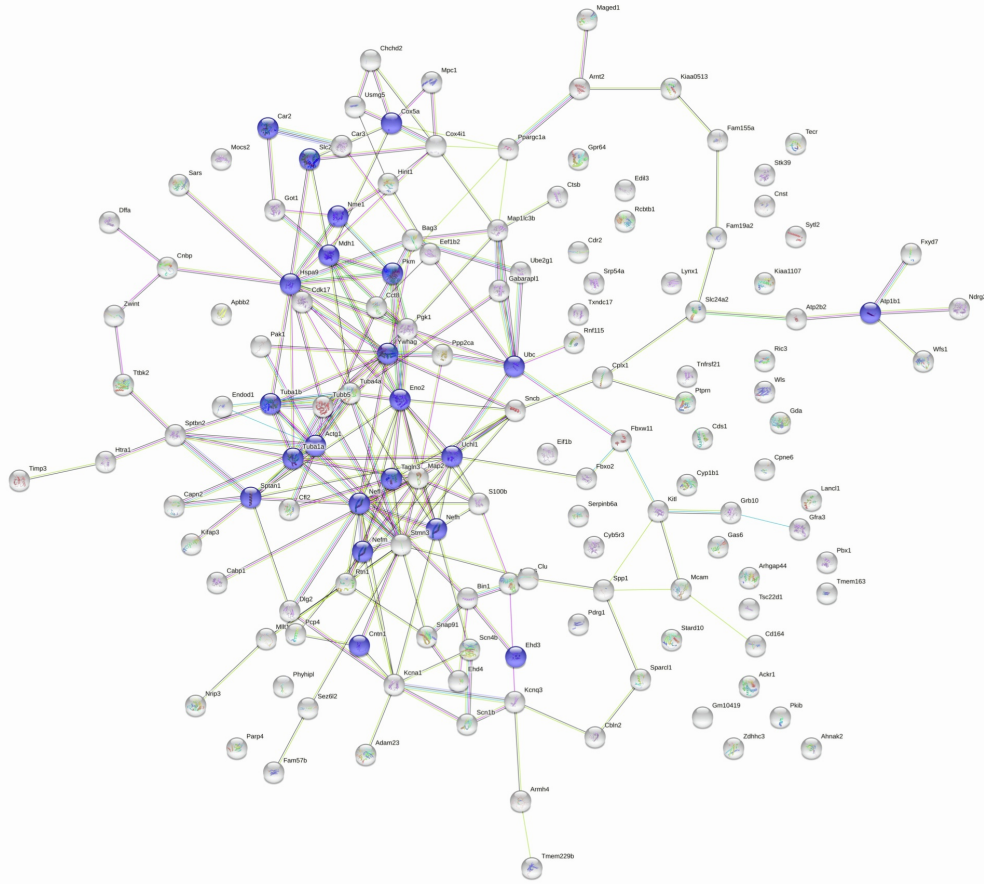
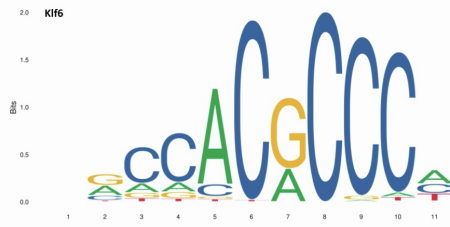
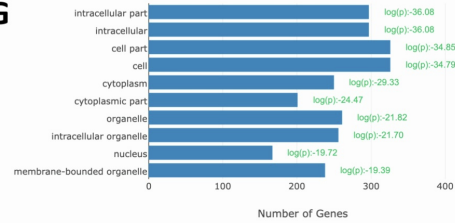
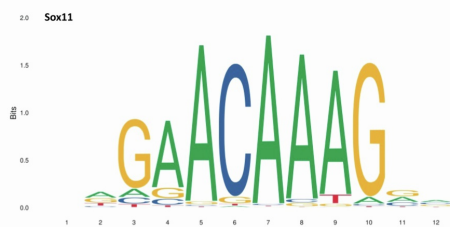
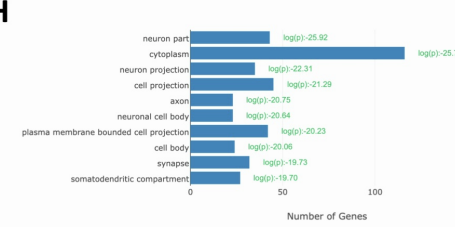
A**B****F****C****G****D****H****E**

Figure S3, related to figure 4. The transcriptional response of neurons to demyelination.

(A) Network analysis of genes induced in neurons only upon demyelination, generated by STRING (Szklarczyk et al., 2015). The most significantly enriched cellular component was myelin sheath, with false discovery rate of 2.02×10^{-16} . Purple nodes denoted “myelin sheath component” proteins and first shell of interactors; white nodes denote second shell of interactors. (B-F) Gene set motif enrichment analysis. The genes induced only by demyelination were enriched for (B) Motif MA1517.1.KLF6 (Relative enrichment ratio 2.13, p -value 3.92×10^{-3} , q -value 2.55×10^{-2}) and (C) Motif MA0605.1.Atf3 (Relative enrichment ratio 1.2, p -value 6.57×10^{-3} , q -value 2.85×10^{-2}). The genes induced by only by SpNT were enriched for (D) Motif MA0869.2.Sox11 (Relative enrichment ratio 1.49, p -value 9.88×10^{-3} , q -value 1.43×10^{-2}), (E) Motif MA1988.1.Atf3 (Relative enrichment ratio 1.73, p -value 2.04×10^{-5} , q -value 6.64×10^{-5}) and (F) Motif MA0489.2.Jun (Relative enrichment ratio 1.88, p -value 1.99×10^{-4} , q -value 4.32×10^{-4}) as well as motifs (B) (Relative enrichment ratio 1.35, p -value 1.39×10^{-6} , q -value 6.04×10^{-6}) and (C) (Relative enrichment ratio 1.18, p -value 7.60×10^{-4} , q -value 1.23×10^{-3}). The genes induced by both, SpNT and demyelination were enriched for motif (C), (Relative enrichment ratio 1.92, p -value 1.07×10^{-3} , q -value 6.94×10^{-3}). (G). Cellular component analysis of the genes induced only by SpNT. (H). Cellular component analysis of the genes induced by both demyelination and SpNT.

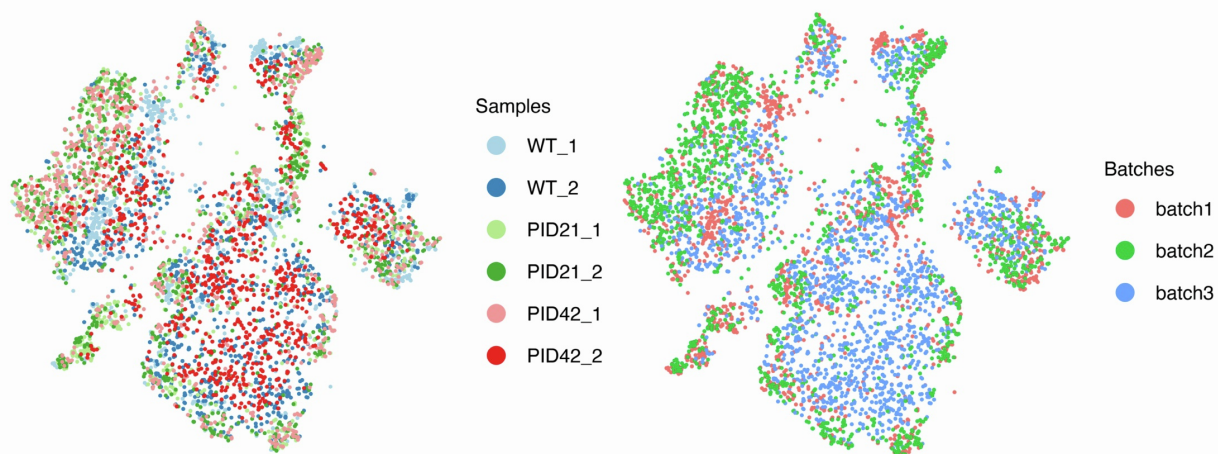
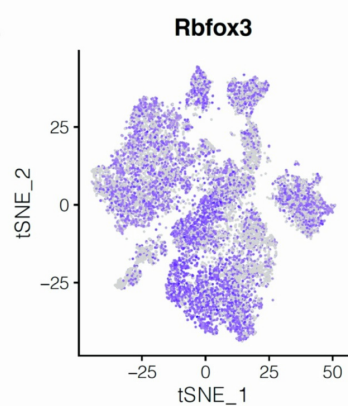
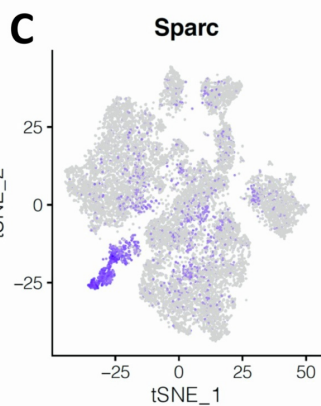
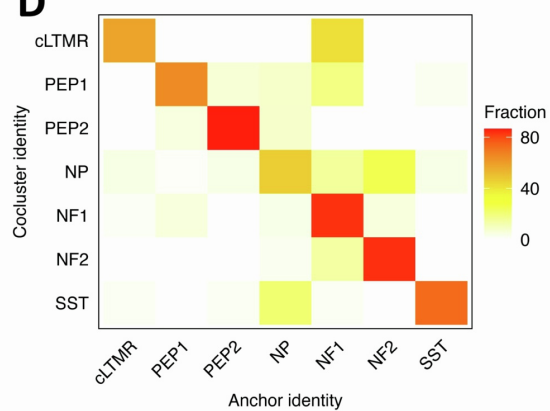
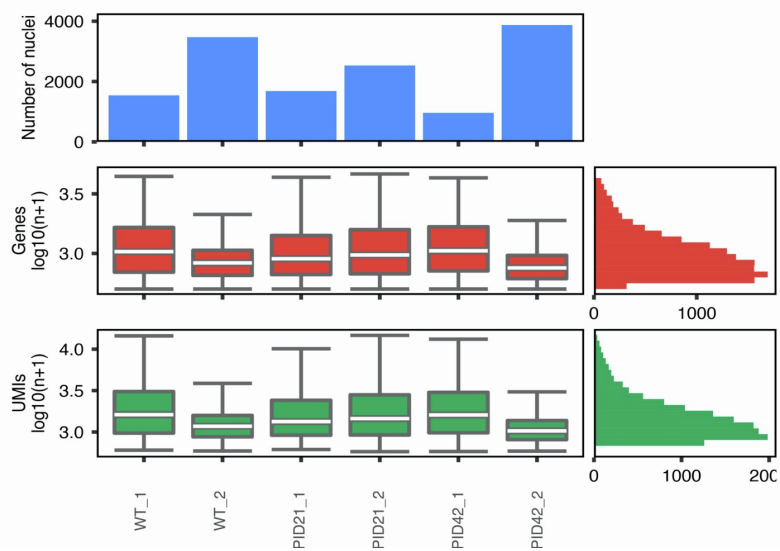
A**B****C****D****E**

Figure S4: snRNA-seq metrics for all sequencing samples. (A) tSNE plot of the nuclei derived from three biological replicates of the experimental conditions. Nuclei are colored by their biological replicate. Each cluster has a mix of nuclei from each replicate, suggesting there are minimal if any batch effects between replicates. (B and C) tSNE plots of the neuronal cluster expressing *Rbfox3*, and non-neuronal clusters expressing *Sparc*. Nuclei are colored by their log₂ expression of the neuronal marker gene *Rbfox3* (B) and non-neuronal marker gene, *Sparc* (C). (D) Overlap of cell type classifications of injured nuclei between coclustering with Spinal Nerve Transection (from Figure 4A) and anchoring to the uninjured clusters (See methods). The fraction of injured nuclei within the initial cell type assignment that is assigned to each cell type after anchoring is displayed. (E). Number of nuclei from each library with > 500 unique genes (top box). Box plots display number of genes per nucleus (log₁₀ transformed, middle row), and unique molecular identifiers (UMI) per nucleus (log₁₀ transformed, bottom row). Boxes indicate quartiles and whiskers are 1.5-times the interquartile range (Q1-Q3). The median is a white line inside each box. The distribution is aggregated across all samples and displayed on the horizontal histogram.